

CD41⁺ cmyb⁺ precursors colonize the zebrafish pronephros by a novel migration route to initiate adult hematopoiesis

Julien Y. Bertrand*, Albert D. Kim*, Shutian Teng and David Traver[†]

Development of the vertebrate blood lineages is complex, with multiple waves of hematopoietic precursors arising in different embryonic locations. Monopotent, or primitive, precursors first give rise to embryonic macrophages or erythrocytes. Multipotent, or definitive, precursors are subsequently generated to produce the adult hematopoietic lineages. In both the zebrafish and the mouse, the first definitive precursors are committed erythromyeloid progenitors (EMPs) that lack lymphoid differentiation potential. We have previously shown that zebrafish EMPs arise in the posterior blood island independently from hematopoietic stem cells (HSCs). In this report, we demonstrate that a fourth wave of hematopoietic precursors arises slightly later in the zebrafish aorta/gonad/mesonephros (AGM) equivalent. We have identified and prospectively isolated these cells by *CD41* (*itga2b*) and *cmyb* expression. Unlike EMPs, *CD41*⁺ AGM cells colonize the thymus to generate *rag2*⁺ T lymphocyte precursors. Timelapse imaging and lineage tracing analyses demonstrate that AGM-derived precursors use a previously undescribed migration pathway along the pronephric tubules to initiate adult hematopoiesis in the developing kidney, the teleostean equivalent of mammalian bone marrow. Finally, we have analyzed the gene expression profiles of EMPs and AGM precursors to better understand the molecular cues that pattern the first definitive hematopoietic cells in the embryo. Together, these studies suggest that expression of *CD41* and *cmyb* marks nascent HSCs in the zebrafish AGM, and provide the means to further dissect HSC generation and function in the early vertebrate embryo.

KEY WORDS: Hematopoiesis, Hematopoietic stem cells, Zebrafish

INTRODUCTION

Generation of blood cells in the vertebrate embryo is a dynamic process, with different anatomical locations transiently hosting different waves of hematopoiesis. It was initially believed that all hematopoietic activity in the murine embryo ultimately derived from hematopoietic stem cells (HSCs) born in the extra-embryonic yolk sac (Moore and Metcalf, 1970). Subsequent hematopoietic sites were thus thought to instruct different fate outcomes from migrating precursors related by lineage. Later experiments, first in birds (Dieterlen-Lievre, 1975; Le Douarin et al., 1975) then in mice (Muller et al., 1994; Cumano et al., 1996; Medvinsky and Dzierzak, 1996), demonstrated that HSCs were generated autonomously within the embryo proper in a region bounded by the aorta, gonads and mesonephros (AGM). These results suggested that different hematopoietic sites are required to independently derive different, or redundant, subsets of hematopoietic precursors from mesoderm.

In the zebrafish, the development of hematopoietic cells also proceeds through multiple embryonic locations. The first functional hematopoietic cells are embryonic macrophages that derive from cephalic mesoderm and begin migrating throughout the embryo by 18 hours post-fertilization (hpf) (Herbomel et al., 1999). Concomitant with macrophage maturation, bilateral stripes of *gata1*⁺ cells converge to the midline, forming a structure termed the intermediate cell mass (ICM) (Al-Adhami and Kunz, 1977). This axial band of erythroid precursors is then enveloped by endothelial cells of the developing cardinal vein, through which they enter circulation upon initiation of heart contractions at ~24 hpf (Detrich,

3rd et al., 1995). These first two waves of embryonic hematopoiesis have been termed primitive. This nomenclature is consistent with findings in mammals, where both primitive macrophages and erythrocytes develop in the yolk sac without passing through a multipotent progenitor stage (Keller et al., 1999; Palis et al., 1999; Bertrand et al., 2005a; Bertrand et al., 2005b).

In contrast to adult hematopoiesis, where committed progenitors are the progeny of HSCs, embryonic hematopoiesis generates committed progenitors before HSCs can be detected. Definitive, or multilineage, hematopoiesis initiates with the formation of committed erythromyeloid progenitors (EMPs) in the posterior blood island (PBI) of the zebrafish embryo at ~24 hpf (Bertrand et al., 2007). EMPs exist only transiently, and like their counterparts recently described in the murine yolk sac (Palis et al., 1999; Cumano et al., 2001; Bertrand et al., 2005c; Yokota et al., 2006), lack lymphoid and self-renewal potential.

Embryonic hematopoiesis culminates with the formation of HSCs, the first multipotent precursors endowed with lymphoid and self-renewal potentials (Cumano et al., 1996; Delassus and Cumano, 1996; Bertrand et al., 2005c). Precisely where and when the first HSCs are born in the mammalian embryo remains controversial. Cells capable of long-term, multilineage reconstitution (LTR) of transplanted recipient animals have been isolated from murine embryonic day (E) 9 yolk sac (Weissman, 1978; Yoder et al., 1997a; Yoder et al., 1997b), E9 para-aortic splanchnopleura (P-Sp; the precursor of the AGM region) (Yoder et al., 1997b; Cumano et al., 2001), E11 AGM (Muller et al., 1994; Medvinsky and Dzierzak, 1996) and E11 placenta (Gekas et al., 2005; Ottersbach and Dzierzak, 2005). Furthermore, recent experiments have demonstrated multilineage hematopoietic activity in the murine allantois and chorion before circulation and before these tissues fuse to become the placenta (Zeigler et al., 2006). Taken together, these results demonstrate the complexity of HSC formation and suggest that the generation of mammalian HSCs may occur de novo in several embryonic locations.

Section of Cell and Developmental Biology, Division of Biological Sciences, University of California, San Diego, La Jolla, CA 92093-0380, USA.

*These authors contributed equally to this work

[†]Author for correspondence (e-mail: dtraver@ucsd.edu)

Accepted 27 March 2008

In the zebrafish embryo, cells expressing the HSC-associated genes *cmyb* and *runx1* have been observed between the ventral wall of the dorsal aorta and the cardinal vein between 28 and 48 hpf (Thompson et al., 1998; Burns et al., 2002; Kalev-Zylinska et al., 2002). Based on the similarities to other vertebrate AGM regions, these cells have been presumed to be the first HSCs to arise in the zebrafish. Until recently, however, functional data have been lacking. Lineage tracing studies demonstrated that the ventral aortic region contained cells with hematopoietic potential, the progeny of which colonized the thymus and the pronephros, the sites of adult hematopoiesis (Murayama et al., 2006; Jin et al., 2007). More recently, we have shown by lineage tracing that CD41⁺ (*itga2b*⁺ – Zebrafish Information Network) EMPs in the PBI between 30 and 40 hpf lacked thymic population potential, whereas CD41⁺ cells targeted along the ventral aortic wall displayed robust thymic colonization (Bertrand et al., 2007). Subsequent studies by Herbolme and colleagues (Kissa et al., 2008) confirmed that CD41⁺ cells from the zebrafish AGM first colonized the developing thymus, a hallmark of embryonic HSCs in other vertebrate species (Moore and Owen, 1967; Owen and Ritter, 1969; Jotereau et al., 1980; Jotereau and Le Douarin, 1982; Delassus and Cumano, 1996; Jaffredo et al., 2003). These findings suggest that HSCs are indeed present in the zebrafish AGM equivalent and, like murine AGM HSCs (Ferkowicz et al., 2003; Mikkola et al., 2003; Bertrand et al., 2005c), can be identified by expression of CD41.

In the present study, we used *CD41:eGFP* (Lin et al., 2005) and *cmyb:eGFP* (North et al., 2007) transgenic animals to isolate and characterize prospectively the first HSCs generated in the zebrafish embryo. CD41⁺ cells colonized the thymus following purification by flow cytometry and isochronic transplantation into wild-type recipient embryos. The behavior of CD41⁺ or *cmyb*⁺ cells was also observed by lineage tracing analyses and timelapse microscopy. Our studies reveal a previously undescribed HSC migration pathway from the AGM to the developing pronephros along the pronephric tubules. Quantitative polymerase chain reaction (QPCR) analyses show gene expression profiles specific to EMPs and HSCs. These studies provide the means to identify and discriminate between hematopoietic stem and progenitor cells by anatomic location, gene expression and function.

MATERIALS AND METHODS

Zebrafish stock and embryos

Zebrafish were manipulated as previously described (Westerfield, 1994). Transgenic lines *Tg(gata1:DsRed)* (Traver et al., 2003), *Tg(CD41:eGFP)* (Lin et al., 2005), *Tg(cmyb:eGFP)* (North et al., 2007) and *Tg(rag-2:eGFP)* (Langenau et al., 2003) were used. Hereafter transgenic lines will be referred to without the *Tg(XXX:XXX)* nomenclature for clarity.

Whole-mount RNA in situ hybridization

Whole-mount RNA in situ hybridization was performed as previously described (Thisse et al., 1993; Bertrand et al., 2007).

Fluorescence-activated cell sorting (FACS)

Whole or dissected embryos were dissociated at 30, 42, 65 or 72 hpf and processed for cellular dissociation and flow cytometry as previously described (Bertrand et al., 2007).

Hematopoietic cell transplantation

CD41:eGFP⁺gata1:DsRed⁻ cells were prepared and sorted as described above and transplanted into 72 hpf wild-type (WT) embryos as previously described (Traver et al., 2003).

Real-time quantitative polymerase chain reaction (QPCR)

For QPCR analyses, RNA was isolated using the RNeasy Kit (Qiagen, Valencia, CA), and cDNA obtained using a SuperscriptIII RT-PCR kit (Invitrogen, Philadelphia, PA). QPCR reactions were performed using the Mx3000P System according to the manufacturer's instructions (Stratagene, La Jolla, CA). Each sample was tested in triplicate. In independent experiments, elongation factor 1 α (*ef1a*) expression was measured for each population and used to normalize signals for each queried transcript using the $\Delta\Delta C_t$ method. These data were normalized to whole kidney marrow (WKM) expression, defined as 100% for all analyses. Primers were designed with Primer3 software (Rozen and Skaletsky, 2000) (Table 1).

Fate-mapping and lineage tracing

One- to eight-cell stage *CD41:eGFP* transgenic embryos were injected with 0.5 nl of a 0:1 or 1:1 mix of caged fluorescein-dextran 10,000 and caged rhodamine-dextran 10,000 (Molecular Probes, Carlsbad, CA). Uncaging was performed using a 365 nm Micropoint laser system (Photonic Instruments, St Charles, IL). Five or ten GFP⁺ target cells were uncaged per embryo using laser pulses of 10–20 seconds each. Uncaged rhodamine-dextran cells were observed by fluorescence microscopy, whereas uncaged FITC was detected by immunohistochemistry, as described previously (Murayama et al., 2006). *CD41:eGFP*, *Rag-2:eGFP* embryos were injected with caged rhodamine in thymus co-expression experiments.

Imaging and microscopy

Embryos were imaged as described previously (Bertrand et al., 2007).

silent heart morpholino injections

A silent heart (tmt2 – Zebrafish Information Network) morpholino (Sehnert et al., 2002) (4 ng) was injected into the cell of *cmyb:eGFP* zygotes. Morphants were visualized daily by fluorescence microscopy.

Generation of *Tg(CD45:DsRed)* and *Tg(gata3:AmCyan)* transgenic animals

A 7.6 kb fragment immediately upstream of the *CD45* transcriptional start site was cloned from the bacmid DKEY-47C5 by PCR into the pDsRed-Express-1 vector (Clontech, Mountain View, CA) using the following primers: *CD45-FP*, CTACTGTATGGACAGAAGACCTGAATC; and *CD45-RP*, TCCAAAAGTTCAAACGCCCTCTTC. A 2 kb fragment immediately upstream of the *gata3* transcriptional start site was cloned from

Table 1. QPCR primers

Gene	Forward primer	Reverse primer
<i>ef1a</i>	GAGAAGTTCGAGAAGGAAGC	CGTAGTATTTGCTGGTCTCG
<i>gata1</i>	TGAATGTGTGAATTGTGGTG	ATTGCGTCTCCATAGTGTG
<i>pu.1</i>	AGAGAGGGTAACCTGGACTG	AAGTCCACTGGATGAATGTG
<i>mpx</i>	TGATGTTTGGTTAGGAGGTG	GAGCTGTTTTCTGTTTGGTG
<i>cmyb</i>	CCGACAGAAGCCGGATGA	TGGCACTTCGCCTCAACTG
<i>lmo2</i>	AAATGAGGAGCCGGTGGAT	GCTCGATGGCCTTCAGAAA
<i>CD45</i>	AGTTCCTGAAATGGAAAAGC	GCACAGAAAAGTCCAGTACG
<i>c-mpl</i>	CGCCAACCAAAGCCAGAGTTA	ACTTTTCAACAGGTGCATCCCA
<i>gata3</i>	CTGATAGGTGGTCTCTTC	CCGTTTCATCTTGTTGTAAG
<i>runx1</i>	CGGTGAACGGTTAATATGAC	CTTTTCATCACGGTTTATGC
<i>CD41</i>	CTGAAGGCAGTAACGTCAAC	TCCTTCTTCTGACCACACAC
<i>ncam</i>	CTTTATCAAGCAGGACGATG	GGTTTTCTGCAATGACGTAG

the bacmid BX901908 by PCR into the pAmCyan-N1 vector (Clontech). The primers used were: *gata3-FP*, GTATAGTTTTTCGGGGCGGCTTC; and *gata3-RP*, TCACCGATACACACAACACG. Transgenic constructs were excised and ligated into Tol2 transgenesis vectors (Kawakami et al., 2004). Resulting constructs were co-injected with Tol2 mRNA into one-cell stage embryos to generate transgenic founders. A *gata-3:AmCyan* transgenic line with expression specific to the pronephric tubules was used in this study.

RESULTS

Definitive hematopoietic cells arise along the aorta by 30 hpf

We recently reported that definitive hematopoiesis initiates with the formation of committed erythromyeloid progenitors (EMPs) in the PBI between 24 and 30 hpf (Bertrand et al., 2007). Our results demonstrate that EMPs arise de novo in the PBI, but exist only as transient precursors, probably disappearing by 48 hpf. Based on the appearance of thymus colonizing cells in the PBI after 40 hpf (Bertrand et al., 2007), and on recent lineage tracing results (Murayama et al., 2006; Jin et al., 2007), HSCs appear to seed the PBI to maintain hematopoiesis in this region, which expands to become caudal hematopoietic tissue (CHT) (Murayama et al., 2006) after 36 hpf. We therefore wished to determine when and where these presumptive HSC immigrants are born. To assess the presence of hematopoietic progenitors in the embryo, we performed whole-mount in situ hybridization using probes for pan-leukocyte *CD45* (*ptprc* – Zebrafish Information Network) and HSC-associated *cmyb* transcripts from 24–72 hpf. Based on *CD45* expression, hematopoietic cells are present in the nascent PBI at 24 hpf (Fig. 1A), consistent with our previous observations of EMP formation in this region (Bertrand et al., 2007). Expression in the AGM, which we define as the region dorsal to the yolk-tube extension that is bounded by the axial vessels and pronephric tubules, initiated slightly later, from ~30–36 hpf (Fig. 1B–E). By comparison, expression of *cmyb* was observed slightly earlier in the AGM, from ~27 hpf onwards (Fig. 1G–J). *cmyb* is therefore an earlier marker of AGM hematopoietic precursors than *CD45*, consistent with findings in the mouse AGM (Bertrand et al., 2005c; Matsubara et al., 2005).

A *CD41:eGFP* transgene marks definitive precursors in the AGM

CD41 has been described as the earliest surface marker of committed definitive precursors in the mouse (Mitjavila-Garcia et al., 2002; Ferkowicz et al., 2003; Mikkola et al., 2003; Bertrand et al., 2005c; Yokota et al., 2006). Our previous observations of transgenic *CD41:eGFP* zebrafish embryos showed the presence of rare GFP⁺ cells scattered between the aorta and the vein in 48 hpf embryos (Lin et al., 2005). Here, we have expanded upon these observations to show that CD41⁺ cells are present as early as 27 hpf in the trunk of the embryo, appearing to arise randomly between the axial vessels (Fig. 2). After this time, CD41⁺ cells expand in number throughout the AGM (Fig. 2J–N).

CD41⁺ cells were also observed bilaterally along each pronephric tubule (Fig. 2F–I). Appearance of ductal, GFP⁺ cells were visible from ~32 hpf (Fig. 2F), and GFP⁺ cells increased in number over time, until ~30–40 GFP⁺ cells per duct were observed by 48 hpf (Fig. 2G). In contrast to GFP⁺ cells between the axial vessels, which displayed either a spindle-shaped or spherical morphology, GFP⁺ cells along the pronephric ducts appeared flattened (Fig. 2F–I). In addition, timelapse microscopy demonstrated dynamic behavior of CD41⁺ cells within the AGM. Lateral views of the AGM region in *CD41:eGFP* animals from 48 to 55 hpf showed GFP⁺ cells to migrate from between the axial vessels to the pronephric ducts, often

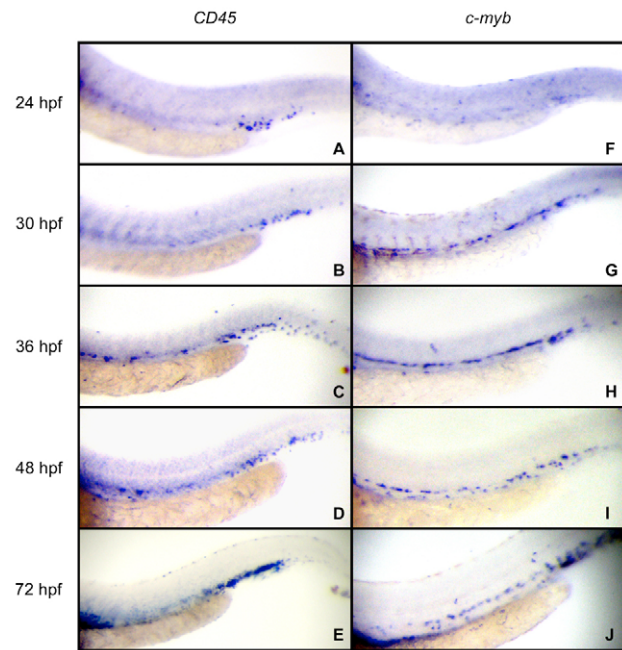


Fig. 1. Expression of *CD45* and *cmyb* marks regions of definitive hematopoiesis in the zebrafish embryo. (A–E) *CD45* expression initiates in the PBI by 24 hpf. (B) By 30 hpf, occasional cells begin to appear between the axial vessels in the AGM (ventral to the yolk tube extension). (C–E) Robust expression is observed in both the PBI/CHT and AGM regions from 36 hpf onwards. (F–J) *cmyb* expression marks cells within the AGM slightly before *CD45* is expressed. (H–J) After 36 hpf, *cmyb* expression is observed in a similar pattern to *CD45* throughout the AGM and CHT. All animals are displayed anterior towards the left and dorsal side upwards.

quickly returning to the vessel region (see Movie 1 in the supplementary material). In addition, CD41⁺ cells were observed to seed the thymic lobes as early as 48 hpf (Fig. 2C; see Movie 2 in the supplementary material). Numbers of CD41⁺ cells peaked in the thymus between 72 and 80 hpf (Fig. 2D) before developing thymocytes lost expression of the CD41 transgene (Fig. 2E). Examination of *cmyb:eGFP* transgenic embryos (North et al., 2007) showed similar patterns of expression (see Fig. S1 in the supplementary material). *cmyb*⁺ cells were first apparent between the axial vessels in the AGM at 27 hpf (see Fig. S1J in the supplementary material), within the developing thymus by 48 hpf (see Fig. S1C in the supplementary material), and along the pronephric tubules by 32 hpf (see Fig. S1F in the supplementary material). Together, these expression patterns suggest that GFP transgenes driven by the *CD41* or *cmyb* promoters label similar populations of hematopoietic precursors in the AGM region.

Transplanted CD41⁺ precursors colonize the thymus and caudal hematopoietic tissue

Antibodies against the CD41 receptor have been extensively used to purify and transplant hematopoietic precursors from the mouse embryo (Mitjavila-Garcia et al., 2002; Ferkowicz et al., 2003; Mikkola et al., 2003; Bertrand et al., 2005c; Yokota et al., 2006). In order to test the homing potentials of zebrafish CD41⁺ AGM cells functionally, we performed similar prospective isolation approaches using *CD41:eGFP*; *gata-1:DsRed* double transgenic embryos. *CD41⁺gata-1⁻* cells were isolated by flow cytometry from 72 hpf

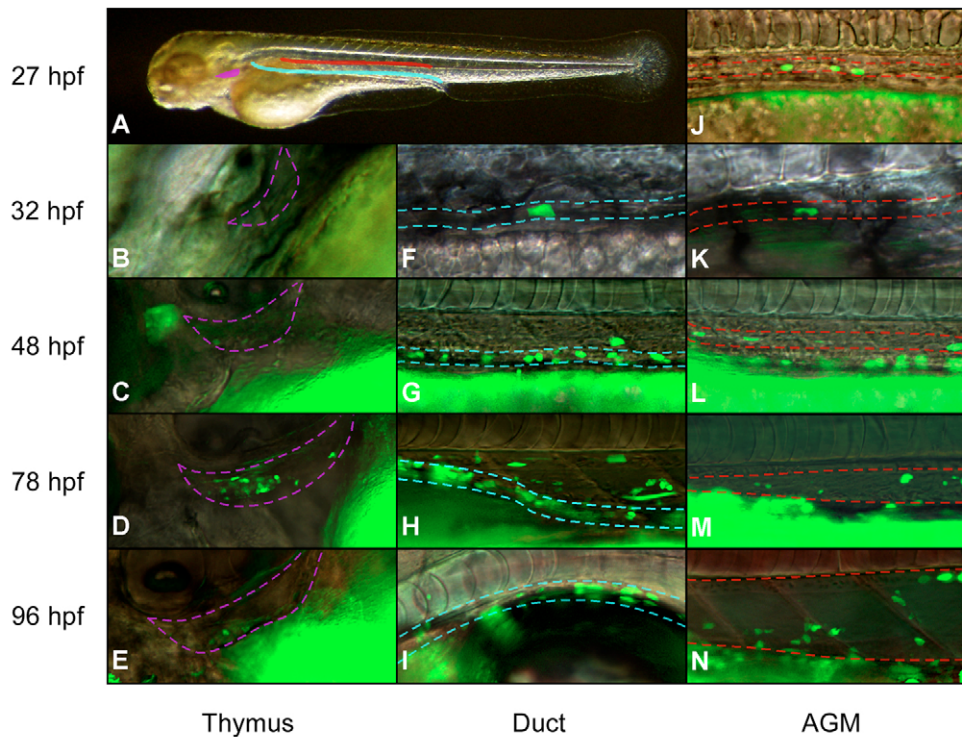


Fig. 2. A *CD41:eGFP* transgene marks cells in the AGM, along the pronephric ducts and in the thymic lobes. (A) Overview of regions shown at higher magnification in fluorescent images. Purple region denotes left thymic lobe, blue region the left pronephric tubule and red region the AGM (space between axial vessels). (B–E) *CD41* is expressed in the first thymic immigrants at ~48 hpf. *GFP*⁺ cells increase in number until 78 hpf, after which *GFP* expression disappears. (F–I) *GFP*⁺ cells appear along the pronephric tubules beginning at ~32 hpf, and increase in number over time. Broken lines indicate the boundaries of the duct. (J–N) *GFP*⁺ cells are first observed in the AGM region at ~27 hpf, and increase in number over time. After 48 hpf, the AGM region greatly expands as the aorta and vein move apart. The upper broken line denotes the ventral wall of the dorsal aorta, the lower line the dorsal wall of the cardinal vein. *GFP*⁺ ductal cells appear ventrolateral to cells within the demarcated AGM region. Images are Nomarski/fluorescence merges. Embryos positioned anterior towards the left and dorsal side upwards.

embryos and transplanted into aged-matched wild-type embryos. One day after injection, we observed robust colonization of host thymic and caudal hematopoietic tissues (Fig. 3A,B) by donor-derived cells. Based on lineage tracing of cells along the aorta, it has previously been suggested that HSCs may migrate from the AGM to colonize the CHT (Murayama et al., 2006; Jin et al., 2007). Our transplantation results support this hypothesis in that the majority of donor-derived cells appear within the CHT 1 day after intravenous injection, and many appear to differentiate rapidly there, based on upregulation of the *gata-1:DsRed* transgene (Fig. 3D). That *CD41*⁺ cells from the AGM can populate the thymus suggests that these cells are markedly different from EMPs that arise earlier in the PBI. We were concerned that the transplanted cells that populated the thymus may have come from existing thymic immigrants in the donor embryos. We therefore transplanted *CD41*⁺ cells from dissected embryonic trunks to remove potentially contaminating thymic residents. We obtained similar results to whole embryo transplants, with donor cells colonizing the CHT and thymic lobes (not shown). Thus, the *CD41:eGFP* transgene marks cells in the AGM region with the ability to colonize definitive hematopoietic organs in transplant recipients.

Lineage tracing demonstrates that *CD41*⁺ cells seed the thymus from the AGM

As an independent test of lymphoid potential, a hallmark of AGM HSCs in mammals (Delassus and Cumano, 1996), we employed laser uncaging of caged fluorescent compounds in AGM

CD41:eGFP⁺ cells. This strategy allowed us to test whether *GFP*⁺ cells between the trunk axial vessels, and their daughters, have the ability to populate the thymus, while bypassing possible harmful effects from sorting and transplantation. *GFP*⁺ cells in *CD41:eGFP* embryos previously injected with caged-rhodamine were targeted at 40 hpf using a microscope-based UV laser. Approximately 10 cells were targeted in each embryo, either *GFP*⁺ cells between the axial vessels in the AGM or *GFP*⁻ cells outside of the AGM as negative controls. Unlike *CD41:eGFP*⁺ EMPs in the PBI that never showed thymic repopulation potential before 40 hpf (Bertrand et al., 2007), *CD41*⁺ cells targeted in the AGM robustly populated the thymic lobes in 10/16 embryos (Fig. 4A).

We next wished to determine whether these thymic immigrants were lymphoid. We therefore performed uncaging experiments using animals carrying two transgenes, *CD41:eGFP* and *Rag-2:eGFP*. *GFP* expression from the lymphoid-specific *Rag2* promoter is never observed within the AGM region in single transgenic embryos (J.Y.B. and D.T., unpublished). Within the thymus, there is also little overlap in *GFP* expression between the two transgenes in double transgenic animals. Expression from the *CD41* promoter disappeared from the thymus by 5 dpf (Fig. 4B, left panel), whereas *GFP* expression from the *Rag2* promoter initiates in the thymus around 4 dpf (Fig. 4B, right panel). To determine whether *rag2*⁺ cells are the descendants of *CD41*⁺ cells in the AGM, we uncaged rhodamine in 10 *CD41*⁺ cells at 40 hpf and analyzed thymic cells after 5 dpf in double transgenic animals. We observed robust clusters of rhodamine⁺ cells that expressed the *Rag-2:eGFP*

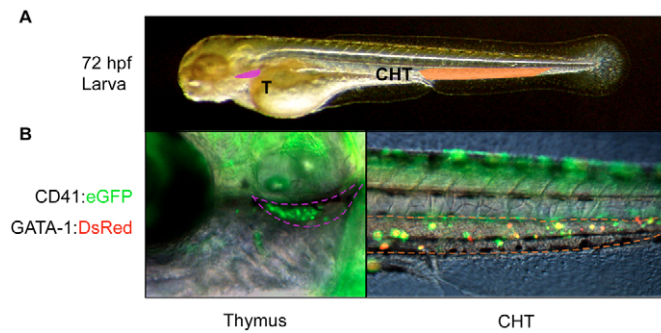


Fig. 3. Transplanted *CD41:eGFP*⁺ cells colonize the thymus and caudal hematopoietic tissues. (A) Photograph indicating regions shown at higher magnification in B (Nomarski/fluorescence merge). Purple region denotes left thymic lobe and orange region the CHT. (B) One day after transplantation, recipient animals showed robust colonization of thymi (left panel) and the CHT (right panel). Transplanted *CD41*⁺ cells also carried a *gata1:DsRed* transgene to visualize erythroid differentiation.

transgene in 5/6 targeted double transgenic embryos (Fig. 4C). In addition, confocal microscopy demonstrated rhodamine⁺ cells migrated to the thymus along ductal structures, and became *Rag2:eGFP*⁺ upon reaching the thymic interior (Fig. 4D). Together, our results suggest that *CD41*⁺ cells in the AGM immigrate to the thymus where they differentiate into T lymphocyte precursors, similar to classic findings on colonization of the thymus in mouse, quail and chick embryos by immature hematopoietic precursors (Moore and Owen, 1967; Owen and Ritter, 1969; Jotereau et al., 1980; Jotereau and Le Douarin, 1982).

AGM *CD41*⁺ cells display a gene expression pattern unique to HSCs

We, and others, have previously shown that *CD41* is expressed by definitive hematopoietic precursors, EMPs and HSCs, respectively, originating from the yolk sac or AGM in the mouse embryo (Bertrand et al., 2005c; Yokota et al., 2006), and the PBI or AGM in the zebrafish embryo (Bertrand et al., 2007). Based on their differing functional attributes, we wished to assess the gene expression profiles of purified EMPs and AGM *CD41*⁺ cells. We purified EMPs at 30 hpf by co-expression of *lmo2:eGFP* and *gata1:DsRed* transgenes, as described (Fig. 5A,B) (Bertrand et al., 2007). To exclude EMPs in the PBI, *CD41*⁺ cells were purified from the AGM following dissection of embryonic trunks (Fig. 5C). In addition, we chose a 42 hpf timepoint to minimize potential contamination by lymphoid-committed progenitors as the thymus has not been colonized at this time (Fig. 2 and data not shown). We performed QPCR to compare the expression of genes enriched in hematopoietic stem and progenitor cells. As expected, the EMP population expressed *gata1* and *pu.1* (*spi1* – Zebrafish Information Network), transcription factors that act as master regulators of erythroid and myeloid fate commitment, respectively, in hematopoietic progenitor cells (Tenen et al., 1997; Miyamoto et al., 2002; Rosenbauer and Tenen, 2007). Transcripts for *gata1* and *pu.1* were undetectable in AGM *CD41*⁺ cells (Fig. 5D). Similar results were obtained for *mpx*, a myelomonocytic-specific gene whose transcription is upregulated upon HSC commitment to myeloid precursors (Tenen et al., 1997; Miyamoto et al., 2002; Rosenbauer and Tenen, 2007). Both purified EMPs and *CD41*⁺ cells expressed the *cmyb* and *lmo2* genes, both canonical markers of hematopoietic stem and progenitor cells (Fig.

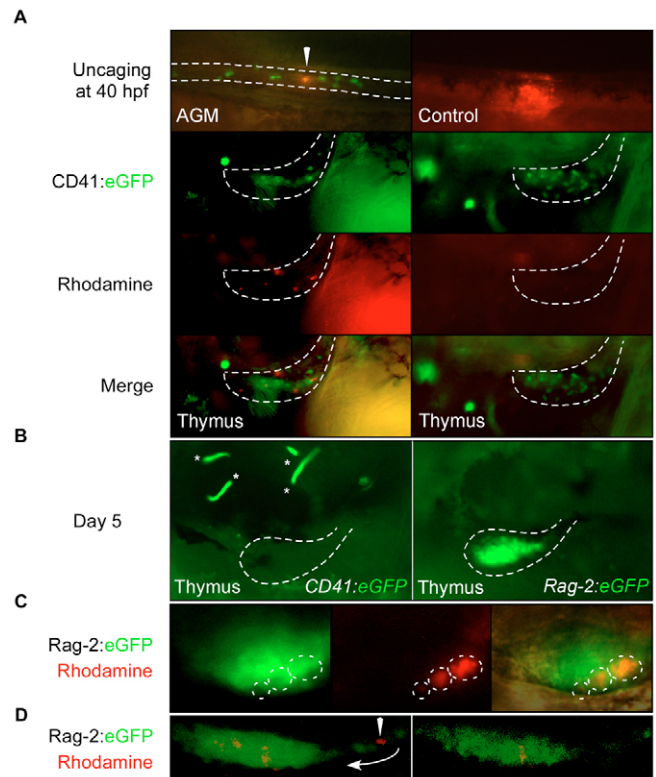


Fig. 4. AGM *CD41:eGFP*⁺ cells seed the thymus to become *rag2*⁺ thymocytes. (A) Upper left panel shows one *CD41:eGFP*⁺ cell immediately after rhodamine uncaging at 40 hpf (arrowhead). Ten cells were uncaged per embryo, and thymic lobes (areas within broken lines in lower panels) were analyzed at 4 dpf. Rhodamine⁺ cells were observed in the thymic lobes, along with GFP⁺ cells that were not uncaged (lower left panel). Control animals where regions outside of the AGM were laser uncaged never showed rhodamine⁺ thymic cells (right panels). (B–D) Similar uncaging experiments using *CD41:eGFP*, *Rag-2:eGFP* double transgenic animals show labeled thymic immigrants are lymphoid. (B) *CD41:eGFP*⁺ cells were laser targeted at 40 hpf in the AGM and thymi analyzed at 5 dpf, when thymic cells no longer express the *CD41* transgene (left panel; asterisks mark circulating *CD41*⁺ thrombocytes) and when nascent thymocytes robustly express the *rag2* transgene (right panel). (C) Targeted *CD41:eGFP*⁺ cells migrate to the thymus and express the *rag2* transgene. Left panel shows GFP expression in a representative thymic lobe, middle panel clones of rhodamine⁺ cells and right panel a merged imaged, including Nomarski overlay. (D) Confocal imaging of targeted thymic immigrants. Left panel shows a maximum projection of the entire thymic lobe, and shows a rhodamine⁺ GFP[−] cell migrating (arrowhead) into the thymus via a posterior thymic duct (arrow). Right panel shows a single z-slice through the thymus showing expression of GFP and rhodamine. All embryos oriented dorsal side upwards, anterior towards the left.

4B) (Orkin, 1996). Expression was uniformly lower in *CD41*⁺ cells than in purified EMPs. Expression of *CD45*, a pan-leukocyte antigen, was found at very low levels in both EMPs and AGM cells when compared with whole kidney marrow (WKM). *CD45* is known to be a relatively late marker of HSCs in the developing murine AGM (Bertrand et al., 2005c; Matsubara et al., 2005). Low-level expression may thus reflect recent commitment from mesodermal derivatives in both populations. Low levels of *c-mpl* (*mpll* – Zebrafish Information Network), the thrombopoietin receptor, were also observed in both populations, with AGM cells

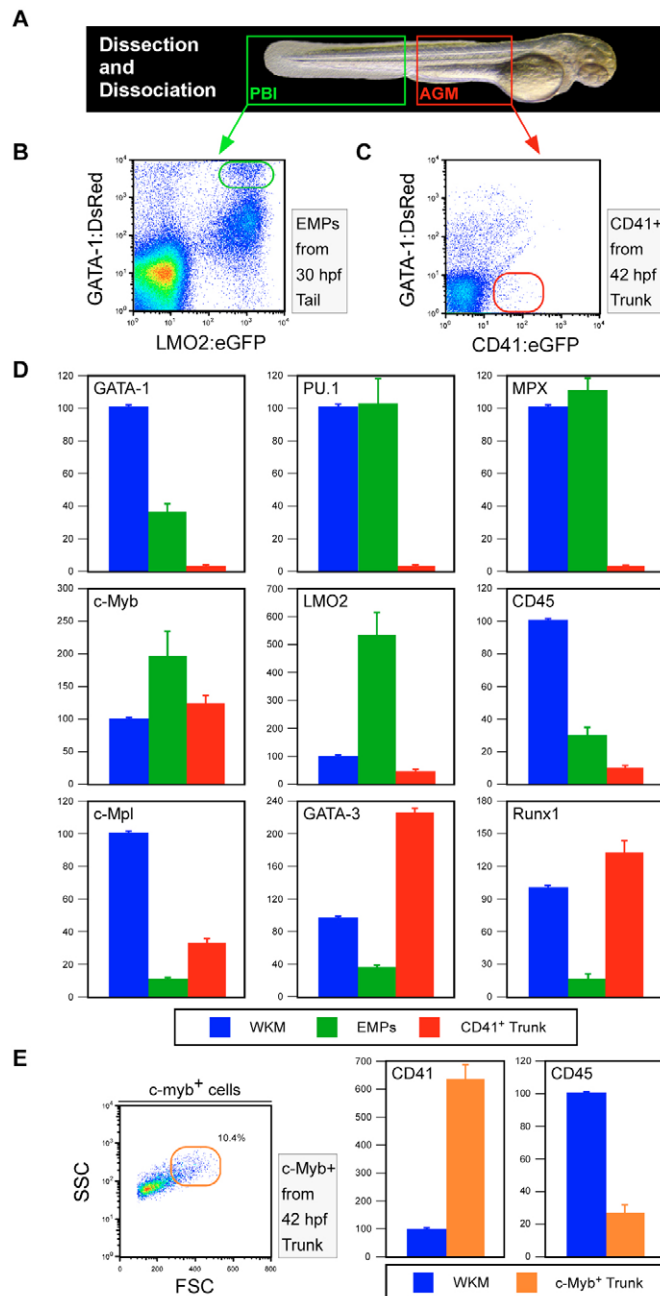


Fig. 5. Comparison of gene expression profiles between purified AGM cells and EMPs. (A) PBI (green box) or AGM (red box) regions were dissected from embryos at 30 or 42 hpf, respectively. (B) EMPs were purified from PBI preparations by flow cytometry based on co-expression of *gata1:DsRed* and *lmo2:eGFP* transgenes (green gate). (C) Presumptive HSCs were purified from AGM preparations by flow cytometry based on *CD41:eGFP⁺gata1:DsRed⁻* expression (red gate). (D) QPCR was performed for a variety of lineage-affiliated genes. Whole-kidney marrow (WKM; blue bars) was used as the reference standard for all analyses of EMP (green bars) and CD41⁺ trunk cell expression (red bars). (E) *cmyb⁺FSC^{hi}* trunk cells (orange gate) were purified from dissected trunks of 42 hpf *cmyb:eGFP* embryos for QPCR analyses (orange bars).

showing approximately twofold higher levels than EMPs. By contrast, *c-mpl* was highly expressed in CD41⁺ cells sorted from 42 hpf tails (not shown), suggesting that this population is enriched for

thrombocyte precursors at this stage, consistent with previous analyses of the *CD41:eGFP* animal (Lin et al., 2005). In addition to the erythromyeloid-affiliated genes, major expression differences between EMPs and HSCs were found for the *gata3* and *runx1* genes (Fig. 5D). AGM cells expressed approximately sixfold higher levels of *gata3* than did EMPs. A similar difference has previously been shown in the mouse embryo between AGM-derived HSCs and yolk sac-derived EMPs (Bertrand et al., 2005c). *gata3* has recently been shown to be a direct target of the Notch signaling pathway (Amsen et al., 2007; Fang et al., 2007). These results may thus reflect active Notch signaling in CD41⁺ cells, which is known to be required to establish *runx1⁺, cmyb⁺* cells in the zebrafish AGM (Burns et al., 2005). Furthermore, *runx1*, a transcription factor required for the development of murine AGM HSCs (Okuda et al., 1996), was expressed at approximately sevenfold higher levels in CD41⁺ AGM cells than in EMPs (Fig. 5D). The gene expression profile of CD41⁺ cells in the AGM, along with the transplantation and fate-mapping studies presented above, support the hypothesis that these cells constitute the primordial HSC population in the developing zebrafish embryo.

As described above, *cmyb:eGFP* animals displayed an expression pattern very similar to that in *CD41:eGFP* animals. We therefore wished to know whether *cmyb⁺* cells also expressed HSC-related genes. We determined that *cmyb⁺* cells could be purified from dissected embryonic trunks by flow cytometry into two populations: one consisting of small agranular cells (*FSC^{lo}*) and the other of larger granular cells (*FSC^{hi}*; see Fig. S2A,B in the supplementary material). Consistent with neuronal GFP expression in smaller cells within the spinal cord (see Fig. S2A in the supplementary material), purified *FSC^{lo}* cells expressed relatively high levels of the neural cell adhesion molecule (*ncam*) gene when compared with both whole 5 dpf embryos and purified *FSC^{hi}* cells (supplementary material Fig. S2C). Conversely, *FSC^{hi}* cells expressed the hematopoietic-specific *CD45* gene, whereas the *FSC^{lo}* subset did not (see Fig. S2C in the supplementary material). The *cmyb⁺, FSC^{hi}* fraction was further analyzed for *CD41* expression and found to express this definitive hematopoietic precursor marker at approximately sixfold higher levels than in WKM (Fig. 5E). These experiments demonstrate that the *CD41* and *cmyb* GFP transgenes mark at least partially overlapping subsets of definitive hematopoietic precursor cells within the AGM.

A *CD45:DsRed* transgene labels a subset of CD41⁺ AGM cells and differentiated leukocytes

Since our whole-mount in situ hybridization analyses suggested that *CD45* was expressed in AGM HSCs, we generated a *CD45:DsRed* transgenic animal to enable more precise study of early hematopoiesis. *DsRed* expression was observed in all described regions of embryonic leukocyte production, including the rostral blood island, posterior blood island and AGM (not shown). Generation of double transgenic *CD45:DsRed, CD41:eGFP* animals demonstrated that a subset of GFP⁺ cells in the AGM co-expressed *DsRed* (see Fig. S3A in the supplementary material). After 5 dpf, expression was observed in the thymic lobes (not shown) and regions of the developing pronephric glomeruli (see Fig. S3B in the supplementary material). Overall, expression of *DsRed* in *CD45:DsRed* transgenic animals closely recapitulated the endogenous expression pattern of *CD45* (Fig. 1), suggesting that it serves as an accurate marker of zebrafish leukocytes, similar to that shown for mammalian *CD45* (Woodford-Thomas and Thomas, 1993).

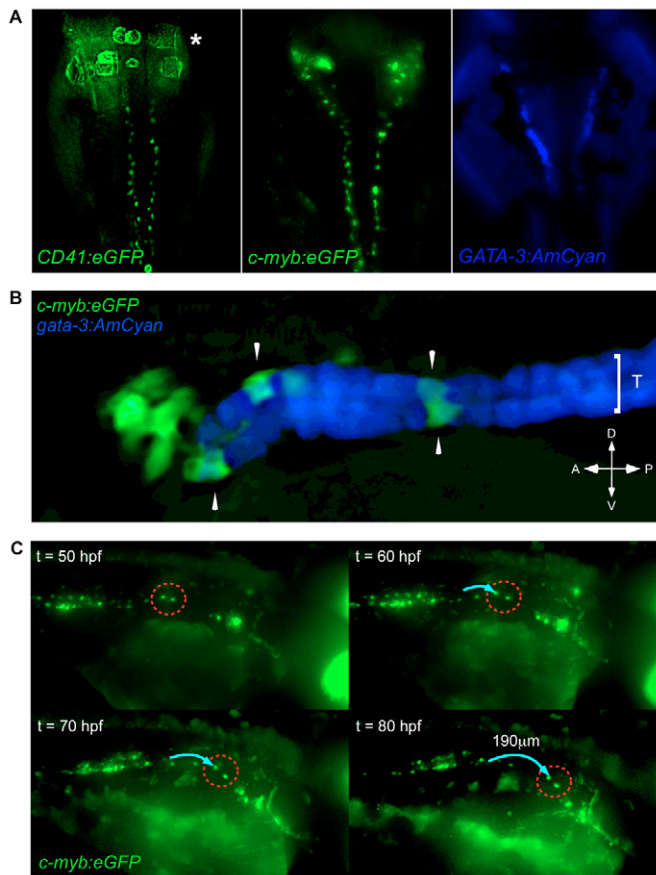


Fig. 6. Hematopoietic precursors migrate along the pronephric tubules. (A) *CD41:eGFP* (left panel; asterisk marks fluorescence from circulating thrombocytes) and *cmyb:eGFP* (middle panel) transgenes are expressed in cells along each pronephric tubule. The anterior pronephric tubules are marked by a *gata3:AmCyan* transgene (right panel). Dorsal views of animals with anterior side upwards. (B) *cmyb:eGFP*⁺ cells (arrowheads) are localized upon *gata3:AmCyan*⁺ pronephric tubules (T). (C) Timelapse imaging demonstrates *cmyb:eGFP*⁺ cells migrate along the pronephric tubules in an anterior direction. Two GFP⁺ cells (dotted red circle) were observed to migrate ~190 μm (blue arrow) over 30 hours. Embryos imaged dorsal side upwards, anterior towards the right.

CD41⁺ *cmyb*⁺ CD45^{low} hematopoietic precursors seed the developing kidney following migration along the pronephric tubules

Timelapse imaging of the AGM region in either *CD41:eGFP* or *cmyb:eGFP* animals from 48-96 hpf showed that GFP⁺ cells moved slowly along each pronephric tubule from the posterior AGM towards the anterior glomeruli (see Movies 3-5 in the supplementary material). The pattern of GFP⁺ cells in either transgenic line appeared similar to fluorescent cells observed in a *gata3:AmCyan* transgenic animal with expression specific to the pronephric tubules (Fig. 6A). This pattern is consistent with previous observations of *gata3* expression in mouse (George et al., 1994; Grote et al., 2006) and zebrafish (Neave et al., 1995; Wingert et al., 2007) pronephric tubules. Analysis of *cmyb:eGFP*; *gata3:AmCyan* double transgenic animals showed that *cmyb*⁺ cells colocalized to *gata3*⁺ pronephric tubules (Fig. 6B). Timelapse analyses of *cmyb:eGFP*⁺ cells over 50-80 hpf demonstrated pronephric migrants moved an average of ~190

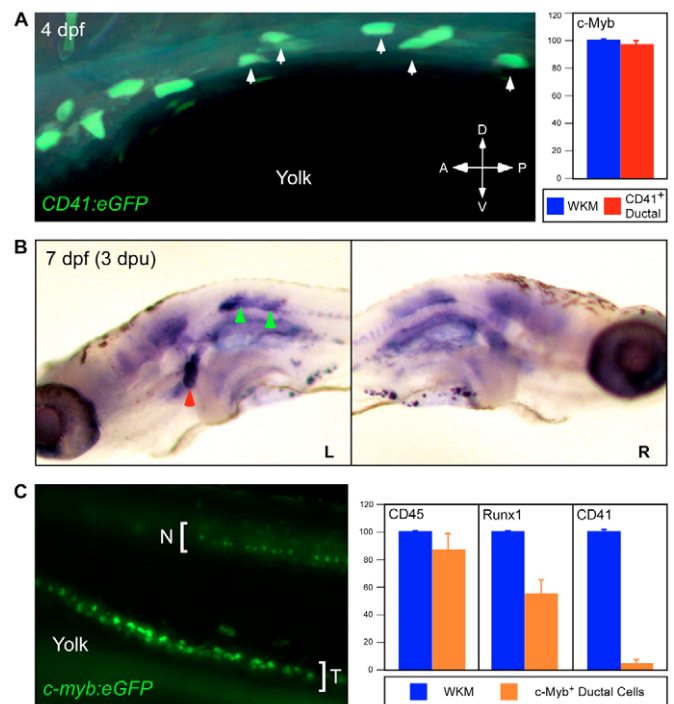


Fig. 7. Characterization of hematopoietic precursors on the pronephric tubules. (A) FITC was uncaged in 5 *CD41:eGFP*⁺ cells (arrows) at 4 dpf along the left pronephric tubule. *CD41:eGFP*⁺ cells express *cmyb* (right panel). (B) Animals were fixed 3 days post-uncaging and analyzed for uncaged FITC. Ductal cells migrated from targeted region on the left pronephric tubule (green arrowheads, left panel) to the left anterior pronephros (red arrowhead). Contralateral anterior pronephri were not colonized (right panel). (C) *cmyb:eGFP*⁺ tubular cells (T) were purified away from GFP⁺ neural cells (N) from 75 hpf dissected trunks by flow cytometry and analyzed for hematopoietic gene expression (right panel).

μm over this 30-hour interval (Fig. 6C). To determine the endpoints of these directed anterior migrations, we performed fate-mapping experiments by targeting CD41⁺ cells along each duct. Five GFP⁺ cells were targeted on one of the two ducts to uncage FITC (Fig. 7A). When embryos were fixed and processed 3 days later, robust colonization of the anterior pronephros was observed (Fig. 7B). Only the pronephric lobe on the side of the duct targeted was colonized (Fig. 7B), and neither thymic lobe was colonized when cells were targeted on or after 3 dpf (Fig. 7B, and not shown). We purified *CD41:eGFP*⁺ cells from dissected 4 dpf embryonic trunks by flow cytometry and showed these cells to express *cmyb* at levels similar to those found in WKM (Fig. 7A), suggesting that *CD41:eGFP* and *cmyb:eGFP* transgenes mark similar cell types on the pronephric tubules. We similarly isolated migrating ductal cells from dissected trunks of *cmyb:eGFP* animals. By 65-75 hpf, GFP expression largely disappeared from cells between the axial vessels and from neuronal cells by this time (Fig. 7C), resulting in excellent purity of sorted ductal cells. Molecular analyses of purified ductal *cmyb*⁺ migrants demonstrated relatively high expression of *CD45* and intermediate expression of *runx1*, when compared with WKM (Fig. 7C). As migrating cells reached the anterior ends of the ducts, CD41 expression was lost (Fig. 7C, see Fig. S3B in the supplementary material). Concomitant with this apparent downregulation of CD41, CD45 expression increased in the anterior pronephros (see Fig. S3B in the supplementary material). In the

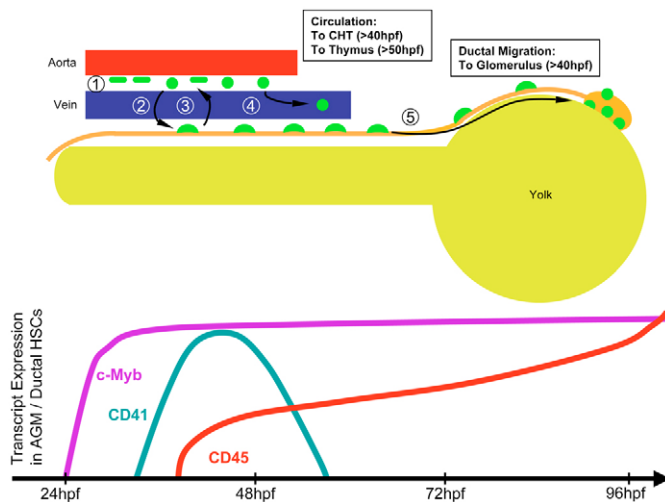


Fig. 8. Model of hematopoietic stem cell migration in the zebrafish embryo. (1) HSCs (green) appear between the dorsal aorta and cardinal vein. (2) Some HSCs translocate to the pronephric tubules (orange) and often back again to between the vessels (3). (4) Some HSCs enter circulation to seed the developing CHT and thymic anlage. (5) HSCs migrate anteriorly along each duct to generate the first hematopoietic cells in the developing kidney. Nascent HSCs can be visualized by expression of the *cmyb*, *CD41* and *CD45* genes (bottom panel).

mouse, CD45 expression has been shown to increase upon hematopoietic differentiation (Bertrand et al., 2005c), suggesting that CD41⁺ hematopoietic precursors mature upon reaching the anterior pronephros. Collectively, our observations suggest that AGM hematopoietic precursors directly initiate T lymphocyte production and kidney hematopoiesis through seeding of the thymic lobes and pronephros, respectively (Fig. 8). Furthermore, our results suggest that the thymus is colonized via HSCs that egress from circulation, whereas the pronephros is seeded through a previously undescribed migration pathway of HSCs along the pronephric ducts. Precursor translocation from between the axial vessels to the ducts occurs independently of circulation, as morpholino knock-down of *silent heart* resulted in no alteration of *cmyb:eGFP* cells along the pronephric tubules (see Fig. S4 in the supplementary material). Eighteen out of 18 morphants displayed normal distribution of GFP⁺ cells along the pronephric tubules (see Fig. S4D,E in the supplementary material); 3/18 morphants displayed rare GFP⁺ cells in the CHT (see Fig. S4F in the supplementary material).

DISCUSSION

We have previously shown that definitive hematopoiesis initiates with the formation of committed erythromyeloid progenitors in the zebrafish PBI around 24 hpf (Bertrand et al., 2007). Here, we show, using a combination of prospective isolation, fate-mapping and imaging approaches, that the first cells with lymphoid potential arise along the dorsal aorta in the zebrafish AGM equivalent beginning at ~27 hpf. Although many previous publications have presumed that HSCs arise in this region, functional studies to verify this hypothesis have been lacking. Two recent lineage tracing studies have demonstrated that cells along the aorta generate progeny that migrate to the CHT, thymus and pronephros (Murayama et al., 2006; Jin et al., 2007), behaviors expected of HSCs. Our results support and refine these studies by demonstrating that the cells responsible for

these hematopoietic colonization events can be identified by CD41 expression that is first apparent between the trunk axial vessels (Fig. 8). AGM CD41⁺ cells generate erythroid progeny in the CHT, *rag2*⁺ T lymphocyte precursors in the thymus, and colonize the pronephros, the adult hematopoietic organ. Collectively, these findings strongly suggest that CD41 expression in the AGM marks the first HSCs in the zebrafish embryo.

Expression of CD41 has been demonstrated to be one of the first markers of mesodermal commitment to the hematopoietic fates in embryonic stem cell models (Mitjavila-Garcia et al., 2002; Mikkola et al., 2003) and during murine embryonic development (Tronik-Le Roux et al., 2000; Ferkowicz et al., 2003; Mikkola et al., 2003; Ottersbach and Dzierzak, 2005). In the zebrafish, expression of CD41 similarly marks commitment to the definitive hematopoietic fates. EMPs born in the PBI express low levels of CD41 beginning at 30 hpf (Bertrand et al., 2007), and presumptive HSCs localized along the dorsal aorta express higher levels, beginning at 27 hpf. It is unclear what functional role CD41 plays on the surface of hematopoietic precursor cells as mutant mice display defects only in platelet function (Tronik-Le Roux et al., 2000) and not in AGM HSC production or function (Emambokus and Frampton, 2003).

The roles of integrins, and other homing and chemoattractant receptors, in the processes of thymic and pronephric colonization by AGM HSCs remain to be determined. Pronephric migrants displayed different morphologies while on the ducts, appearing larger and flatter than CD41⁺ cells in the AGM, which were often observed to fluctuate between small round cells and spindle-shaped cells that frequently intercalated into the ventral wall of the dorsal aorta (see Movie 1 in the supplementary material). Before 3 dpf, timelapse imaging of *CD41:eGFP* animals showed frequent translocations of fluorescent cells between the axial vessels and ducts along the region dorsal to the yolk tube extension. After 3 dpf, ductal CD41⁺ cells were rarely observed to exit the ducts, rather appearing fixed in their directional migration towards the anterior pronephros (see Movie 4 in the supplementary material). Accordingly, our fate-mapping results after 3 dpf showed that CD41⁺ anterior ductal cells (dorsal to the yolk ball) colonized the pronephros only; labeled progeny were not observed in other tissues, including the thymus. Furthermore, donor-derived progeny of transplanted CD41⁺ cells were only rarely detected in the regions of the developing anterior pronephros, whereas transplanted CD41⁺ cells rapidly and robustly seeded the thymic anlage. These results suggest that lymphopoiesis initiates in the thymus upon immigration by blood-borne precursors, in accordance with the recent results of Kissa and colleagues (Kissa et al., 2008). In contrast to the statement by Kissa et al., however, that CD41⁺ cells on the pronephric tubules are not hematopoietic (Kissa et al., 2008), our results demonstrate that ductal *CD41:eGFP*⁺ cells express the hematopoietic-specific *CD45* gene, HSC-affiliated *runx1* and *cmyb* genes, and migrate to the anterior pronephros. When circulation was abolished by a morpholino against the *silent heart* gene, thymi were not seeded by *cmyb:eGFP*⁺ cells, whereas ductal colonization and migration was unaffected. Accordingly, we believe that CD41⁺ *cmyb*⁺ cells initiate hematopoiesis in the zebrafish kidney via a circulation-independent route along the pronephric tubules.

In the murine system, LTR of transplant recipients is the most rigorous assay for HSC function. We performed an extensive number of transplantation experiments using CD41⁺ cells purified from the zebrafish AGM into both wild-type and mutant embryonic recipients. Despite robust colonization of embryonic thymi and CHT, recipient animals showed a uniform loss of donor-derived cells over time. There may be several reasons that AGM cells fail to

provide LTR. The simplest explanation is that CD41⁺ cells in the zebrafish AGM are not HSCs. The similarities of these cells to CD41⁺ HSCs in the murine AGM, the expression of HSC-affiliated genes such as *cmyb*, *runx1* and *gata3* in zebrafish CD41⁺ AGM cells, and the fact that CD41⁺ AGM cells are the first cells in the zebrafish embryo with lymphoid differentiation potential collectively make this possibility unlikely. Unlike the erythroid and myeloid lineages, which first arise from committed hematopoietic precursors independently of HSCs (Palis et al., 1999; Bertrand et al., 2005c; Bertrand et al., 2007), the first cells in the vertebrate embryo with lymphoid differentiation potential are multipotent at the single-cell level (Delassus and Cumano, 1996), and capable of LTR (Bertrand et al., 2005c). It is therefore likely that the CD41⁺ *cmyb*⁺ CD45⁺ cells characterized here are HSCs. Formal validation awaits the development of zebrafish assays able to support LTR from embryonic donor cells.

If establishment of adult hematopoiesis requires HSC immigration to the pronephros via the pronephric tubules, then cells transplanted into circulation may lack the ability to engraft within the teleostean equivalent of mammalian bone marrow. Our previous results using adult kidney cells as donors, however, resulted in LTR (Traver et al., 2003). This suggests either that adult HSCs are markedly different from those in the AGM, or that other factors contribute to the difficulty in achieving LTR using embryonic donor cells. In addition to many transplantation experiments from embryo to embryo, we also transplanted AGM CD41⁺ cells into conditioned adult recipients. Whereas we routinely achieve LTR using adult kidney cells transplanted into sublethally irradiated adult hosts (Traver et al., 2004), we have not observed LTR when using any cell population from embryonic donors. In the mouse, it has been demonstrated that embryonic cells do not express class I MHC molecules before E10.5 (Ozato et al., 1985). The inability of pre-E11 AGM cells, which have been shown to possess multilineage (including lymphoid) differentiation capacity in vitro (Cumano et al., 1996), to engraft adult animals may thus be due to immune rejection via natural killer (NK) cells that are highly radioresistant (Waterfall et al., 1987) and efficiently destroy MHC-I-deficient cells (Lanier, 2005). Surface molecules related to mammalian NK receptors are expressed in zebrafish leukocytes (Panagos et al., 2006), suggesting that improved methods to ablate host NK cells may result in improved donor cell engraftment.

The ontogeny of HSCs has been extensively described in the mouse, where several sites of hematopoiesis may independently generate HSCs. In the zebrafish, we have detected lymphoid potential only from cells in the AGM. In our previous characterization of zebrafish EMPs, we could not detect thymus or pronephros homing potentials from these progenitors born in the PBI. The ICM, the zebrafish equivalent of the yolk sac blood island, forms within the cardinal vein and is thus located just ventral to where CD41⁺ HSCs are first detectable in the narrow region between the cardinal vein and dorsal aorta. As we can currently only detect HSCs by their expression of GFP, it remains to be determined where nascent HSCs arise, and whether they share a common ancestry with primitive erythroid precursors. Likewise, further analyses will be necessary to determine whether HSCs share a common precursor with endothelial cells, as has been previously proposed following experiments in avian (Jaffredo et al., 1998) and murine models (Sugiyama et al., 2003). Our studies in the zebrafish help form the foundation for the continued study of the differences among the embryonic hematopoietic programs, and should lead to a better understanding of the genetic requirements of HSC formation and function in the vertebrate embryo.

We thank Patricia Ernst, Wilson Clements and David Stachura for critical evaluation of the manuscript; Robert Handin for provision of *CD41:eGFP* animals; Leonard Zon for *cmyb:eGFP* animals; Steve Hedrick for QPCR machine use; Karen Ong for assistance with flow cytometry; and Roger Rainville, Evie Wright and Lisa Phelps for excellent animal care. Supported by the Irvington Institute Fellowship Program of the Cancer Research Institute (J.Y.B.), the Stem Cell Research Foundation, National Institutes of Health grant #DK074482, the American Society of Hematology, the March of Dimes Foundation and the Beckman Foundation (D.T.).

Supplementary material

Supplementary material for this article is available at <http://dev.biologists.org/cgi/content/full/135/10/1853/DC1>

References

- Al-Adhami, M. A. and Kunz, Y. W. (1977). Ontogenesis of haematopoietic sites in *Brachydanio rerio*. *Dev. Growth Differ.* **19**, 171-179.
- Amsen, D., Antov, A., Jankovic, D., Sher, A., Radtke, F., Souabni, A., Busslinger, M., McCright, B., Gridley, T. and Flavell, R. A. (2007). Direct regulation of Gata3 expression determines the T helper differentiation potential of Notch. *Immunity* **27**, 89-99.
- Bertrand, J. Y., Giroux, S., Cumano, A. and Godin, I. (2005a). Hematopoietic stem cell development during mouse embryogenesis. *Methods Mol. Med.* **105**, 273-288.
- Bertrand, J. Y., Jalil, A., Klaine, M., Jung, S., Cumano, A. and Godin, I. (2005b). Three pathways to mature macrophages in the early mouse yolk sac. *Blood* **106**, 3004-3011.
- Bertrand, J. Y., Giroux, S., Golub, R., Klaine, M., Jalil, A., Boucontet, L., Godin, I. and Cumano, A. (2005c). Characterization of purified intraembryonic hematopoietic stem cells as a tool to define their site of origin. *Proc. Natl. Acad. Sci. USA* **102**, 134-139.
- Bertrand, J. Y., Kim, A. D., Violette, E. P., Stachura, D. L., Cisson, J. L. and Traver, D. (2007). Definitive hematopoiesis initiates through a committed erythromyeloid progenitor in the zebrafish embryo. *Development* **134**, 4147-4156.
- Burns, C. E., DeBlasio, T., Zhou, Y., Zhang, J., Zon, L. and Nimer, S. D. (2002). Isolation and characterization of *runx* and *runx*b, zebrafish members of the runt family of transcriptional regulators. *Exp. Hematol.* **30**, 1381-1389.
- Burns, C. E., Traver, D., Mayhall, E., Shepard, J. L. and Zon, L. I. (2005). Hematopoietic stem cell fate is established by the Notch-Runx pathway. *Genes Dev.* **19**, 2331-2342.
- Cumano, A., Dieterlen-Lievre, F. and Godin, I. (1996). Lymphoid potential, probed before circulation in mouse, is restricted to caudal intraembryonic splanchnopleura. *Cell* **86**, 907-916.
- Cumano, A., Ferraz, J. C., Klaine, M., Di Santo, J. P. and Godin, I. (2001). Intraembryonic, but not yolk sac hematopoietic precursors, isolated before circulation, provide long-term multilineage reconstitution. *Immunity* **15**, 477-485.
- Delassus, S. and Cumano, A. (1996). Circulation of hematopoietic progenitors in the mouse embryo. *Immunity* **4**, 97-106.
- Detrich, H. W., 3rd, Kieran, M. W., Chan, F. Y., Barone, L. M., Yee, K., Rundstadler, J. A., Pratt, S., Ransom, D. and Zon, L. I. (1995). Intraembryonic hematopoietic cell migration during vertebrate development. *Proc. Natl. Acad. Sci. USA* **92**, 10713-10717.
- Dieterlen-Lievre, F. (1975). On the origin of haemopoietic stem cells in the avian embryo: an experimental approach. *J. Embryol. Exp. Morphol.* **33**, 607-619.
- Emambokus, N. R. and Frampton, J. (2003). The glycoprotein IIb molecule is expressed on early murine hematopoietic progenitors and regulates their numbers in sites of hematopoiesis. *Immunity* **19**, 33-45.
- Fang, T. C., Yashiro-Ohtani, Y., Del Bianco, C., Knoblock, D. M., Blacklow, S. C. and Pear, W. S. (2007). Notch directly regulates Gata3 expression during T helper 2 cell differentiation. *Immunity* **27**, 100-110.
- Ferkowicz, M. J., Starr, M., Xie, X., Li, W., Johnson, S. A., Shelley, W. C., Morrison, P. R. and Yoder, M. C. (2003). CD41 expression defines the onset of primitive and definitive hematopoiesis in the murine embryo. *Development* **130**, 4393-4403.
- Gekas, C., Dieterlen-Lievre, F., Orkin, S. H. and Mikkola, H. K. (2005). The placenta is a niche for hematopoietic stem cells. *Dev. Cell* **8**, 365-375.
- George, K. M., Leonard, M. W., Roth, M. E., Lieu, K. H., Kioussis, D., Grosfeld, F. and Engel, J. D. (1994). Embryonic expression and cloning of the murine GATA-3 gene. *Development* **120**, 2673-2686.
- Grote, D., Souabni, A., Busslinger, M. and Bouchard, M. (2006). Pax 2/8-regulated Gata 3 expression is necessary for morphogenesis and guidance of the nephric duct in the developing kidney. *Development* **133**, 53-61.
- Herbomel, P., Thisse, B. and Thisse, C. (1999). Ontogeny and behaviour of early macrophages in the zebrafish embryo. *Development* **126**, 3735-3745.
- Jaffredo, T., Gautier, R., Eichmann, A. and Dieterlen-Lievre, F. (1998). Intraortic hemopoietic cells are derived from endothelial cells during ontogeny. *Development* **125**, 4575-4583.

- Jaffredo, T., Alais, S., Bollerot, K., Drevon, C., Gautier, R., Guezguez, B., Minko, K., Vigneron, P. and Dunon, D. (2003). Avian HSC emergence, migration, and commitment toward the T cell lineage. *FEMS Immunol. Med. Microbiol.* **39**, 205-212.
- Jin, H., Xu, J. and Wen, Z. (2007). Migratory path of definitive hematopoietic stem/progenitor cells during zebrafish development. *Blood* **109**, 5208-5214.
- Jotereau, F. V. and Le Douarin, N. M. (1982). Demonstration of a cyclic renewal of the lymphocyte precursor cells in the quail thymus during embryonic and perinatal life. *J. Immunol.* **129**, 1869-1877.
- Jotereau, F. V., Houssaint, E. and Le Douarin, N. M. (1980). Lymphoid stem cell homing to the early thymic primordium of the avian embryo. *Eur. J. Immunol.* **10**, 620-627.
- Kalev-Zylinska, M. L., Horsfield, J. A., Flores, M. V., Postlethwait, J. H., Vitas, M. R., Baas, A. M., Crosier, P. S. and Crosier, K. E. (2002). Runx1 is required for zebrafish blood and vessel development and expression of a human RUNX1-CBF2T1 transgene advances a model for studies of leukemogenesis. *Development* **129**, 2015-2030.
- Kawakami, K., Takeda, H., Kawakami, N., Kobayashi, M., Matsuda, N. and Mishina, M. (2004). A transposon-mediated gene trap approach identifies developmentally regulated genes in zebrafish. *Dev. Cell* **7**, 133-144.
- Keller, G., Lacaud, G. and Robertson, S. (1999). Development of the hematopoietic system in the mouse. *Exp. Hematol.* **27**, 777-787.
- Kissa, K., Murayama, E., Zapata, A., Cortes, A., Perret, E., Machu, C. and Herbomel, P. (2008). Live imaging of emerging hematopoietic stem cells and early thymus colonization. *Blood* **111**, 1147-1156.
- Langenau, D. M., Traver, D., Ferrando, A. A., Kutok, J., Aster, J. C., Kanki, J. P., Lin, H. S., Prochownik, E., Trede, N. S., Zon, L. I. et al. (2003). Myc-induced T-Cell leukemia in transgenic zebrafish. *Science* **299**, 887-890.
- Lanier, L. L. (2005). NK cell recognition. *Annu. Rev. Immunol.* **23**, 225-274.
- Le Douarin, N. M., Houssaint, E., Jotereau, F. V. and Belo, M. (1975). Origin of hemopoietic stem cells in embryonic bursa of Fabricius and bone marrow studied through interspecific chimeras. *Proc. Natl. Acad. Sci. USA* **72**, 2701-2705.
- Lin, H. F., Traver, D., Zhu, H., Dooley, K., Paw, B. H., Zon, L. I. and Handin, R. I. (2005). Analysis of thrombocyte development in CD41-GFP transgenic zebrafish. *Blood* **106**, 3803-3810.
- Matsubara, A., Iwama, A., Yamazaki, S., Furuta, C., Hirasawa, R., Morita, Y., Osawa, M., Motohashi, T., Eto, K., Ema, H. et al. (2005). Endomucin, a CD34-like sialomucin, marks hematopoietic stem cells throughout development. *J. Exp. Med.* **202**, 1483-1492.
- Medvinsky, A. and Dzierzak, E. (1996). Definitive hematopoiesis is autonomously initiated by the AGM region. *Cell* **86**, 897-906.
- Mikkola, H. K., Fujiwara, Y., Schlaeger, T. M., Traver, D. and Orkin, S. H. (2003). Expression of CD41 marks the initiation of definitive hematopoiesis in the mouse embryo. *Blood* **101**, 508-516.
- Mitjavila-Garcia, M. T., Cailleret, M., Godin, I., Nogueira, M. M., Cohen-Solal, K., Schiavon, V., Lecluse, Y., Le Pesteur, F., Lagrue, A. H. and Vainchenker, W. (2002). Expression of CD41 on hematopoietic progenitors derived from embryonic hematopoietic cells. *Development* **129**, 2003-2013.
- Miyamoto, T., Iwasaki, H., Reizis, B., Ye, M., Graf, T., Weissman, I. L. and Akashi, K. (2002). Myeloid or lymphoid promiscuity as a critical step in hematopoietic lineage commitment. *Dev. Cell* **3**, 137-147.
- Moore, M. A. and Owen, J. J. (1967). Experimental studies on the development of the thymus. *J. Exp. Med.* **126**, 715-726.
- Moore, M. A. and Metcalf, D. (1970). Ontogeny of the haemopoietic system: yolk sac origin of in vivo and in vitro colony forming cells in the developing mouse embryo. *Br. J. Haematol.* **18**, 279-296.
- Muller, A. M., Medvinsky, A., Strouboulis, J., Grosveld, F. and Dzierzak, E. (1994). Development of hematopoietic stem cell activity in the mouse embryo. *Immunity* **1**, 291-301.
- Murayama, E., Kissa, K., Zapata, A., Mordelet, E., Briolat, V., Lin, H. F., Handin, R. I. and Herbomel, P. (2006). Tracing hematopoietic precursor migration to successive hematopoietic organs during zebrafish development. *Immunity* **25**, 963-975.
- Neave, B., Rodaway, A., Wilson, S. W., Patient, R. and Holder, N. (1995). Expression of zebrafish GATA 3 (gta3) during gastrulation and neurulation suggests a role in the specification of cell fate. *Mech. Dev.* **51**, 169-182.
- North, T. E., Goessling, W., Walkley, C. R., Lengerke, C., Kopani, K. R., Lord, A. M., Weber, G. J., Bowman, T. V., Jang, I. H., Grosser, T. et al. (2007). Prostaglandin E2 regulates vertebrate haematopoietic stem cell homeostasis. *Nature* **447**, 1007-1011.
- Okuda, T., van Deursen, J., Hiebert, S. W., Grosveld, G. and Downing, J. R. (1996). AML1, the target of multiple chromosomal translocations in human leukemia, is essential for normal fetal liver hematopoiesis. *Cell* **84**, 321-330.
- Orkin, S. H. (1996). Development of the hematopoietic system. *Curr. Opin. Genet. Dev.* **6**, 597-602.
- Ottersbach, K. and Dzierzak, E. (2005). The murine placenta contains hematopoietic stem cells within the vascular labyrinth region. *Dev. Cell* **8**, 377-387.
- Owen, J. J. and Ritter, M. A. (1969). Tissue interaction in the development of thymus lymphocytes. *J. Exp. Med.* **129**, 431-442.
- Ozato, K., Wan, Y. J. and Orrison, B. M. (1985). Mouse major histocompatibility class I gene expression begins at midsomite stage and is inducible in earlier-stage embryos by interferon. *Proc. Natl. Acad. Sci. USA* **82**, 2427-2431.
- Palis, J., Robertson, S., Kennedy, M., Wall, C. and Keller, G. (1999). Development of erythroid and myeloid progenitors in the yolk sac and embryo proper of the mouse. *Development* **126**, 5073-5084.
- Panagos, P. G., Dobrinski, K. P., Chen, X., Grant, A. W., Traver, D., Djeu, J. Y., Wei, S. and Yoder, J. A. (2006). Immune-related, lectin-like receptors are differentially expressed in the myeloid and lymphoid lineages of zebrafish. *Immunogenetics* **58**, 31-40.
- Rosenbauer, F. and Tenen, D. G. (2007). Transcription factors in myeloid development: balancing differentiation with transformation. *Nat. Rev. Immunol.* **7**, 105-117.
- Rozen, S. and Skaletsky, H. J. (2000). Primer3 on the WWW for general users and for biologist programmers. In *Bioinformatics Methods and Protocols: Methods in Molecular Biology* (ed. S. Misener and S. A. Krawetz), pp. 365-386. Totowa, NJ: Humana Press.
- Sehner, A. J., Huq, A., Weinstein, B. M., Walker, C., Fishman, M. and Stainier, D. Y. (2002). Cardiac troponin T is essential in sarcomere assembly and cardiac contractility. *Nat. Genet.* **31**, 106-110.
- Sugiyama, D., Ogawa, M., Hirose, I., Jaffredo, T., Arai, K. and Tsuji, K. (2003). Erythropoiesis from acetyl LDL incorporating endothelial cells at the prelever stage. *Blood* **101**, 4733-4738.
- Tenen, D. G., Hromas, R., Licht, J. D. and Zhang, D. E. (1997). Transcription factors, normal myeloid development, and leukemia. *Blood* **90**, 489-519.
- Thisse, C., Thisse, B., Schilling, T. F. and Postlethwait, J. H. (1993). Structure of the zebrafish snail1 gene and its expression in wild-type, spadetail and no tail mutant embryos. *Development* **119**, 1203-1215.
- Thompson, M. A., Ransom, D. G., Pratt, S. J., MacLennan, H., Kieran, M. W., Detrich, H. W., 3rd, Vail, B., Huber, T. L., Paw, B., Brownlie, A. J. et al. (1998). The cloche and spadetail genes differentially affect hematopoiesis and vasculogenesis. *Dev. Biol.* **197**, 248-269.
- Traver, D., Paw, B. H., Poss, K. D., Penberthy, W. T., Lin, S. and Zon, L. I. (2003). Transplantation and in vivo imaging of multilineage engraftment in zebrafish bloodless mutants. *Nat. Immunol.* **4**, 1238-1246.
- Traver, D., Winzler, A., Stern, H. M., Mayhall, E. A., Langenau, D. M., Kutok, J. L., Look, A. T. and Zon, L. I. (2004). Effects of lethal irradiation in zebrafish and rescue by hematopoietic cell transplantation. *Blood* **104**, 1298-1305.
- Tronik-Le Roux, D., Roullot, V., Poujol, C., Kortulewski, T., Nurden, P. and Marguerie, G. (2000). Thrombasthenic mice generated by replacement of the integrin alpha(IIB) gene: demonstration that transcriptional activation of this megakaryocytic locus precedes lineage commitment. *Blood* **96**, 1399-1408.
- Waterfall, M., Rayfield, L. S. and Brent, L. (1987). The role of natural killer cells in resistance to allogeneic and parental hybrid resistance. *Transplantation* **43**, 312-314.
- Weissman, I., Papaioannou, V. and Gardner, R. (1978). Fetal hematopoietic origins of the adult hematomorphous system. In *Differentiation of Normal and Neoplastic Hematopoietic Cells* (ed. B. Clarkson, P. A. Marks and J. E. Till), pp. 33-47. New York: Cold Spring Harbor Laboratory Press.
- Westerfield, M. (1994). *The Zebrafish Book: A Guide for the Laboratory use of Zebrafish (Brachydanio rerio)*. Eugene, OR: University of Oregon Press.
- Wingert, R. A., Selleck, R., Yu, J., Song, H. D., Chen, Z., Song, A., Zhou, Y., Thisse, B., Thisse, C., McMahon, A. P. et al. (2007). The cdx genes and retinoic acid control the positioning and segmentation of the zebrafish pronephros. *PLoS Genet.* **3**, 1922-1938.
- Woodford-Thomas, T. and Thomas, M. L. (1993). The leukocyte common antigen, CD45 and other protein tyrosine phosphatases in hematopoietic cells. *Semin. Cell Biol.* **4**, 409-418.
- Yoder, M., Hiatt, K. and Mukherjee, P. (1997a). In vivo repopulating hematopoietic stem cells are present in the murine yolk sac at day 9.0 postcoitus. *Proc. Natl. Acad. Sci. USA* **94**, 6776.
- Yoder, M. C., Hiatt, K., Dutt, P., Mukherjee, P., Bodine, D. M. and Orlic, D. (1997b). Characterization of definitive lymphohematopoietic stem cells in the day 9 murine yolk sac. *Immunity* **7**, 335-344.
- Yokota, T., Huang, J., Tavian, M., Nagai, Y., Hirose, J., Zuniga-Pflucker, J. C., Peault, B. and Kincade, P. W. (2006). Tracing the first waves of lymphopoiesis in mice. *Development* **133**, 2041-2051.
- Zeigler, B. M., Sugiyama, D., Chen, M., Guo, Y., Downs, K. M. and Speck, N. A. (2006). The allantois and chorion, when isolated before circulation or chorio-allantoic fusion, have hematopoietic potential. *Development* **133**, 4183-4192.